applied sciences

MDPI

Article

A Bipolar Voltage Gain Boost AC-AC Converter Based on Four Switching Transistors

Naveed Ashraf [1], Ghulam Abbas [1,*], Nasim Ullah [2], Sattam Al Otaibi [2], Ahmed Althobaiti [2], Muhammad Zubair [3] and Umar Farooq [4]

[1] Department of Electrical Engineering, The University of Lahore, Lahore 54000, Pakistan; naveed.ashraf@ee.uol.edu.pk
[2] Department of Electrical Engineering, College of Engineering, Taif University, Taif 21944, Saudi Arabia; nasimullah@tu.edu.sa (N.U.); srotaibi@tu.edu.sa (S.A.O.); ahmed.althobaiti@tu.edu.sa (A.A.)
[3] Department of Electrical Engineering, College of Engineering, Majmaah University, Majmaah 11952, Saudi Arabia; m.zubair@mu.edu.sa
[4] Department of Electrical Engineering, University of the Punjab, Lahore 54590, Pakistan; engr.umarfarooq@yahoo.com
* Correspondence: ghulam.abbas@ee.uol.edu.pk

Abstract: In numerous applications, such as the correction of grid voltage during voltage sag or swell events caused by system faults, it is necessary to ensure the stabilization of the output voltage with in-phase and out-phase features. This feature can also be employed in high-voltage-gain AC to DC conversion. AC voltage control schemes with one-stage conversion are viable approaches in this regard as only voltage regulation is needed. This conversion approach has strong potential for such applications as it is simple to realize. The voltage-correcting compensators are connected in series with the lines. The inputs of the AC voltage controllers employed in the voltage-correcting compensators may be connected to the faulty phase or other healthy phases. The number of AC voltage controllers used in a voltage compensator are one and two if its input power is drawn from the faulty and non-faulty phases, respectively. In the latter case, voltage gains and phase adjustment are major problems. There is no such issue in the first approach, where the voltage-correcting controller is connected to the line where the voltage variation is to be corrected. A high voltage gain more than the unity of both voltage polarities is required if the depth level of the correcting voltage is around 50% or more. The size and cost of a voltage-correcting controller depend on the number of switching transistors, as an isolated DC source with a gate-controlling circuit is a mandatory requirement for the switching operation of each transistor. Therefore, in the suggested research, an AC voltage controller having bipolar voltage gain is realized only with four switching transistors and six diodes, which reduces the overall size and cost significantly. The verification of the suggested topology is ensured by obtaining the simulation and real results from Simulink-based and practical-based platforms, respectively.

Keywords: voltage sag; voltage controller; voltage gain; switching transistors; non-inverting features; inverting features; faulty and non-faulty phase

check for updates

Citation: Ashraf, N.; Abbas, G.; Ullah, N.; Otaibi, S.A.; Althobaiti, A.; Zubair, M.; Farooq, U. A Bipolar Voltage Gain Boost AC-AC Converter Based on Four Switching Transistors. *Appl. Sci.* **2021**, *11*, 10254. https://doi.org/10.3390/app112110254

Academic Editor: Alfio Dario Grasso

Received: 22 September 2021
Accepted: 29 October 2021
Published: 1 November 2021

Publisher's Note: MDPI stays neutral with regard to jurisdictional claims in published maps and institutional affiliations.

Copyright: © 2021 by the authors. Licensee MDPI, Basel, Switzerland. This article is an open access article distributed under the terms and conditions of the Creative Commons Attribution (CC BY) license (https://creativecommons.org/licenses/by/4.0/).

1. Introduction

The problem of poor power quality in power systems normally results from the extensive use and integration of renewable energy systems or resources, adverse loading, or the use of a non-linear load at an extensive level. This problem may include voltage fluctuation, imbalance of the voltage in the three-phase system, voltage sags and swells, etc. Among these problems, the voltage sags and swells are critical for loads that are very sensitive to voltage variation. These issues may lead to the missed or incorrect operation of sensitive electronic devices or equipment. To address these issues, the use of flexible AC transmission (FACTS) controllers may offer a possible solution if they are employed as a

dynamic voltage restorer (DVR) [1–3]. The basic principle of protection in these devices is the series injection of voltage between the load and point of common coupling (source or transformer) in the power system. The DVRs may be employed in a DC-link-based system, as shown in Figure 1. The most commonly used configuration of DVR, as illustrated in [4–6], is depicted in Figure 1a, which is based on the use of a voltage source inverter and voltage injection transformer connected in series with the line. The input power of these types of DVRs is taken from DC energy-storing devices such as batteries. The duration of the compensation voltage in these configurations depends on the size and capacity of the energy-storing devices but cannot support longer-duration voltage variations. This issue is addressed and tackled in other configurations for voltage compensation [7,8], as shown in Figure 1b. Here, a front-side AC-DC converter eliminates the use of energy-storing devices, enabling the compensator to deal with the longer-duration problems. In both previously discussed configurations, the use of a bulky DC-link capacitor is mandatory, which has very severe reliability issues. Therefore, these configurations are not suitable for applications where only voltage stabilization is required.

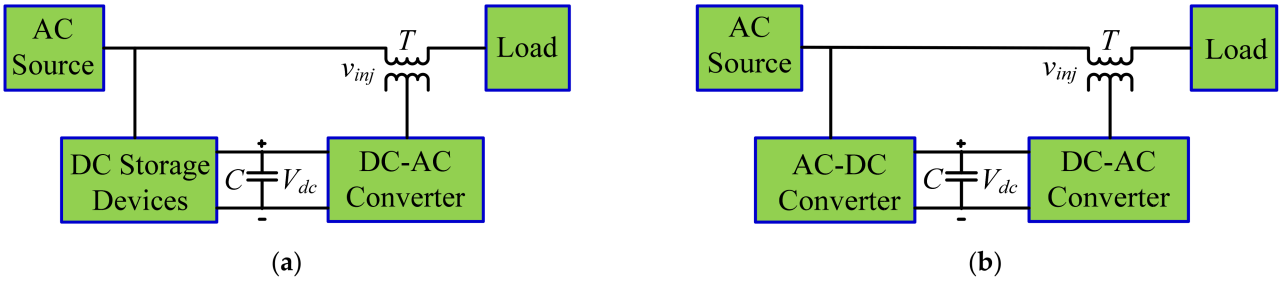

Figure 1. Conventional voltage compensation techniques employed (**a**) with and (**b**) without energy storage devices.

In the other developed approaches of DVRs, the stabilization of the required voltage may be ensured by the PWM control of the direct AC-AC converters [9]. These configurations eliminate the use of a DC-link capacitor; hence, this improves the overall system's reliability. Direct AC-AC topologies may be realized with a Z-source structure [10–14] to increase the capability of the voltage transfer ratio. This also eliminates the risk of short-circuit problems or the paralleling of capacitors connected to input and output terminals. These problems may result from the turning on of the switching transistors connected in series, which must be operated in a complementary way. The usage of a number of passive elements and operating devices is a serious challenge in these power-converting approaches, which is the main cause of their large overall size and cost. The presence of the high-order elements in this arrangement also seriously impacts the dynamic response. There is also an issue of high current stresses conducted in the switching devices during the shoot-through intervals, which increase their power rating, resulting in high costs. These issues are tackled in power-converting approaches implemented without a Z-source configuration, as reported in [15–20]. In these power-converting topologies, an inductor at the intermediate level is employed for energy storage and to avoid the shoot-through issue. The bidirectional current conduction capabilities of the switching MOSFETs in converters [15,17–20] are forced to be unidirectional by connecting a fast recovery at the source end. This arrangement always ensures the reverse biasing or blocking of the conduction of the MOSFET's body diode. This approach not only avoids the shoot-through problem but also simplifies the circuit configuration as well as the switching control techniques. The power quality validation of the AC voltage controllers realized with the direct approach of AC power conversion topologies is explored in [16]. Therefore, these converters are well-suited for the voltage stabilization of a sensitive load in the case of voltage fluctuation.

For low-voltage issues, the rms value of the line voltage is dropped approximately to 80% to 20% of its rated rms values. Thus, to tackle the load voltage, a compensation voltage is added to the line voltage, as shown in Figure 2a. This can only be realized if the

output voltage of a DVR is in phase with the input phase voltage. Therefore, an AC-AC converter has to be operated in non-inverting mode. In the same way, during the voltage swell issue, the line or load rms voltage is increased to 120 to 180% of its rated value. In this case, the compensator's voltage is to be subtracted from the line voltage to stabilize them, as may be seen in Figure 2b. Thus, the required operating mode of the AC-AC compensator employed in DVR is inverting. Consequently, a variable bipolar voltage gain is required to tackle the issues of voltage sag and swell.

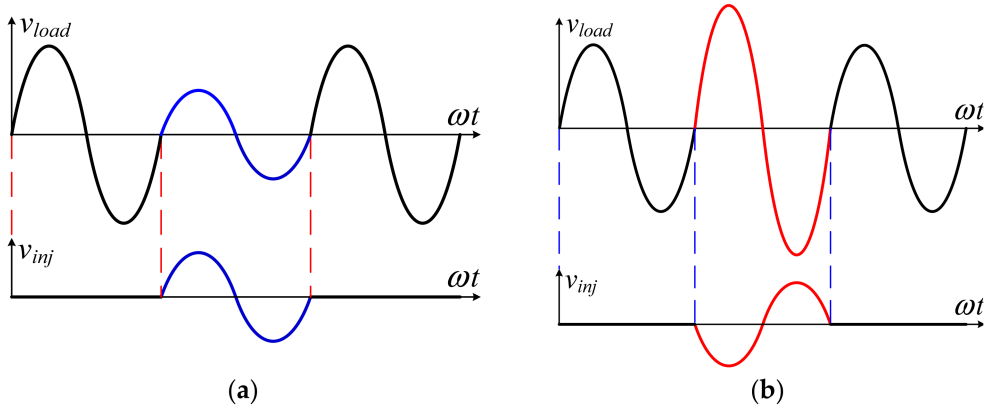

Figure 2. Voltage compensation during (**a**) voltage sag event and (**b**) voltage swell event.

The input of the AC voltage controllers present in the DVRs employed in a three-phase system may be connected in the healthy phases rather than the faulty phase. One such approach is called the interphase technique, developed in [21], which is shown in Figure 3a. The DVR connected in the faulty phase consists of two AC voltage controllers, as depicted in Figure 3b. The input of one AC voltage controller is connected to one of the non-faulty phases, while the input of the other one is taken from the other healthy phase. For example, the inputs of voltage compensator 1 connected in phase '*a*' are connected to phase '*b*' and '*c*', as can be seen in Figure 3a,b. The outputs of these two AC voltage controllers are not only out of phase with respect to each other but are also not aligned with the phase voltage of the faulty line [21]. Here, the voltage injection in the faulty phase is a challenging issue. This problem is tackled by adding the outputs of the two AC voltage controllers through the series connection of two transformers. The resulting output voltage of this setup has two components, where one component is in phase with the voltage of the faulty phase, but the other component is quadrature with respect to this phase. The second component of the injected voltage is unwanted and its value is made zero with the adjustment of the duty cycles of the controllers. Therefore, adjusting the voltage gain of the desired component with the cancelation of the quadrature component is a very challenging issue. Moreover, the use of the two series voltage injection transformers and two AC voltage controllers increases the overall size, cost, and losses.

These issues may be tackled if the AC voltage controller connected in the faulty phase takes the input power from the same phase where it is connected. This approach is depicted in Figure 4, ensuring the use of a single AC-AC converter with a line frequency transformer for voltage injection. The overall arrangement lowers the size and cost of the DVR. However, with this configuration, the value of the required voltage gains for the problem of voltage sag or swell has a high depth level, normally more than one. This necessitates the development of a converter that may invert or non-invert output with voltage step-up capabilities.

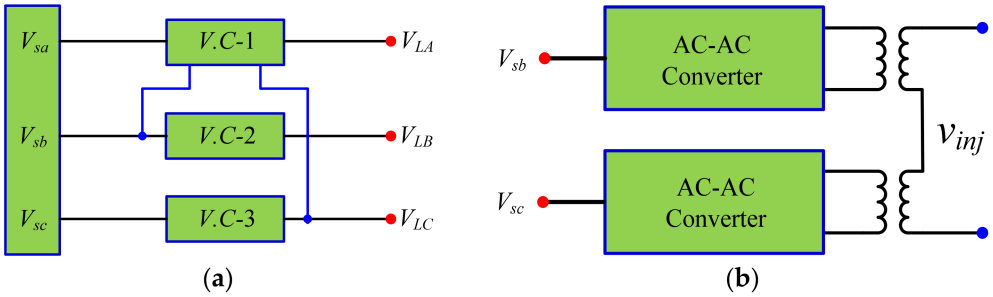

Figure 3. (**a**) Voltage compensation through interphase connection; (**b**) interconnection of AC-AC converters.

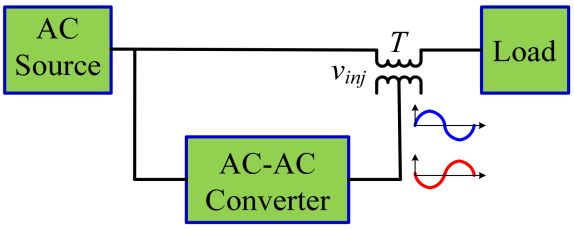

Figure 4. A direct approach of voltage compensation.

The voltage stabilization features may also be obtained with buck-boost controllers. There is a power quality issue associated with the input current as it is discontinuous. High conversion losses result from high values of the switching current and voltage. The discontinuity in the input current is tackled in [22–24] by adding more passive components and semiconductor devices. This may result in high costs and conversion losses due to the conduction of a large number of components and switching devices.

Applications such as line voltage correction having a high depth level or high-voltage-gain AC-to-DC converters need a high bipolar voltage gain. The required features of the voltage gain can be obtained with the realization of voltage boost voltage controllers, which are capable of non-inverting or inverting the input voltage at the output with voltage-regulated characteristics. One of the latest AC voltage controllers having bipolar voltage boost features is employed in [20], as can be viewed in Figure 5.

However, its realization requires the use of six switching transistors and eight diodes. The overall size and cost of any AC voltage controller are directly affected by the use of a number of switching transistors. The switching of one transistor requires the use of one gate-controlling circuit (GCC) with a separate isolated DC source (IDS). The size and cost of a GCC and IDS are much larger than those of a transistor or power converter circuit. The similar existing topologies use a large number of switching transistors (and associated circuits that deal with their turn-on and turn-off control) and diodes, which are the major sources of the increased overall volume, losses, and costs.

Therefore, in this article, a new boost voltage controller having bipolar voltage boost features is proposed that is realized with the use of six diodes and four switching transistors. Therefore, eliminating the number of switching transistors drastically reduces the overall size and cost of the converter. This circuit topology also helps to simplify the switching arrangements, and it also avoids the problems caused by the shoot-through. There is no possibility of interruption of the inductor current that may result from some inherent delay or defect in the operation of the switching transistors. For this purpose, an inductor is connected at the intermediate level to avoid paralleling the input and output capacitors or the shorting of the input or output capacitors. In the same way, the series connection of diode D_5 with transistor Q_4 and diode D_6 with transistor Q_2 helps to tackle the current interruption of the inductor current, which may otherwise lead to the generation of high inductive voltage kicks. With this approach, the transistor Q_2 is ensured to be on for the positive input voltage once the transistor Q_4 operates with high-frequency PWM control.

Once the transistor Q_4 is on, the transistor Q_2 is also on, but it is in the non-conducting state as its series-connected diode is reverse-biased. This diode changes its state from off to on as transistor Q_4 turns off. Thus, the inductor current remains uninterrupted for the PWM switching control for the transistor Q_4. This is also true for the PWM switching control of the transistor Q_2 as well.

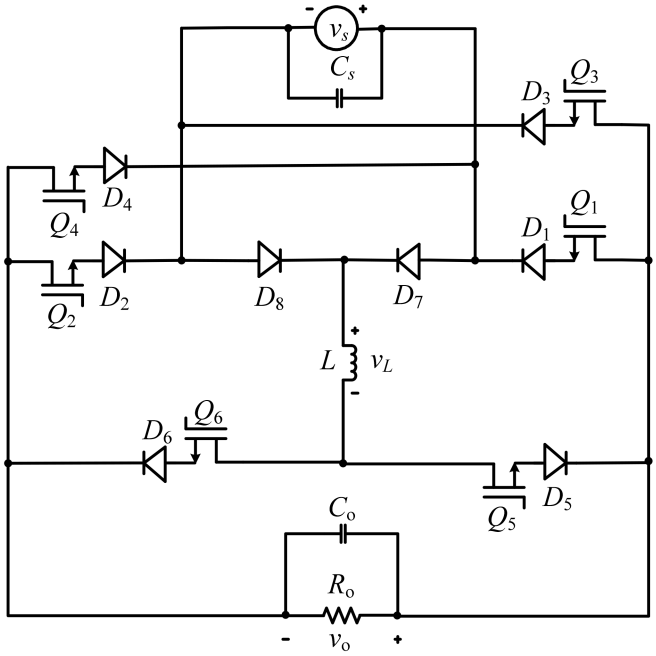

Figure 5. AC voltage controller reported in [20].

The section-wise arrangement of this research article includes the demonstration of all operating modes in Section 2 with the help of power transfer loops and control signals. The effectiveness of the proposed circuit is proven in Section 3 through a comparison with topologies realized with similar strategies. The operational validation of the suggested circuit is carried out in Section 4 with the comparison of results gained from computer software and a practical model. The conclusions are presented in Section 5.

2. Proposed Circuit and Operating Modes

The circuit arrangement of the suggested topology is illustrated in Figure 6. This circuit is a modified form of our developed frequency step-up controller, which is discussed in [25]. The realization of the proposed circuit is achieved with the usage of six fast recovery diodes (D_1 to D_6) and four high switching transistors (Q_1 to Q_4). The switching transistors Q_1 and Q_3 operate at a low frequency (output or input frequency) while transistors Q_2 and Q_4 operate at a high switching frequency (in the kilohertz range). The power quality of the source and load sides is ensured by employing input and output capacitors. The inductor between the diodes and transistor circuits acts not only as a filtering or energy-storing element but also eliminates the possible shorting of the input or output capacitors. It also avoids the paralleling of the input and output capacitors. Therefore, the problem of possible shoot-through that may develop due to inherent turn-off delays of the high-frequency switching transistors is solved. For example, switching transistors Q_1 and Q_4 are connected in series and may operate in a complementary way. There is the possibility that Q_4 may turn on before the Q_1 turns off. In this case, the series-connected inductor (L) prevents the short-circuiting of the input source. The same is also true for transistors Q_3 and Q_4. The current through the series inductor is always unidirectional, and its interruption is avoided with a proper control arrangement developed for the switching of the four transistors. In the same way, the possible shorting of the output capacitor (C_o) is eliminated by connecting the diode

D_5 in series with transistor Q_4 and diode D_6 in series with transistor Q_2. This connection arrangement ensures the reverse blocking of the body diodes of the switching transistors Q_4 and Q_2. There is no need to connect the series diodes with switching transistor Q_1 and Q_3 to ensure the reverse biasing of their body diodes. Here, the polarity of the output capacitor will perform this task. For example, once the switching transistor Q_1 is on and Q_3 is off, the negative terminal of the output capacitor is connected to the anode of the body diode of the switching transistor Q_3. The same is also true once the switching transistor Q_3 is on and transistor Q_1 is off. The suggested topology and its non-inverting and inverting voltage boost capabilities are detailed in the next section with the help of voltage control schemes and power transfer loops.

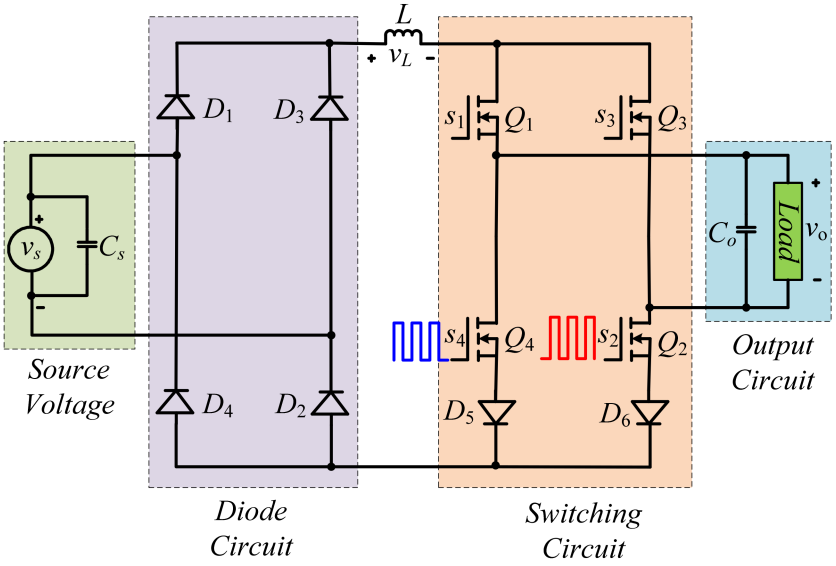

Figure 6. Proposed circuit topology.

The regulated non-inverted and inverted output voltage is a mandatory requirement for stabilizing the load voltage during the problem of voltage sag and swell. The voltage of the output compensator must be added and subtracted from the load voltage in the event of voltage sag and swell issues, respectively. This requires non-inverting and inverting outputs with voltage-regulated characteristics. The diode bridge converts the sinusoidal input to its absolute form, while the transistor bridge ensures the regulated sinusoidal voltage at the output. The required regulated AC output is ensured with the switching of four transistors (Q_1 to Q_4). The inductor (L) and output capacitor (C_o) are passive energy-storing elements, so they may be employed as state variables to explore the dynamic behavior.

2.1. Voltage Control with Non-Inverting Characteristics

In this mode, the regulated voltage with boost characteristics and input voltage are in phase with each other. This output voltage feature may be ensured with control algorithms, as shown in Figure 7a. In this figure, v_{zcd} is the output of a voltage-sensing circuit that detects the polarity of the input voltage. This voltage is logically high and low once the input voltage waveform passes through the positive and negative cross-over points, respectively. This is applied to the signal generator (microcontroller) as input; thus, all the control outputs of the signal generator are synchronized or aligned with the grid AC voltage. The control voltages v_{s1} and v_{s3} ensure the on states of the switching transistors Q_1 and Q_3 once the input voltage has positive and negative values. Similarly, the control voltage v_{s4} and v_{s2} are high-frequency PWM signals that switch transistors Q_4 and Q_2, respectively. These control signals operate the switching transistors in a pulse width modulation (PWM) manner when the input voltage is positive and negative, respectively,

to stabilize the output according to the requirement. The maximum off-state voltage across the turned-off switching transistors (Q_1 to Q_4) is restricted to the peak value of the output voltage.

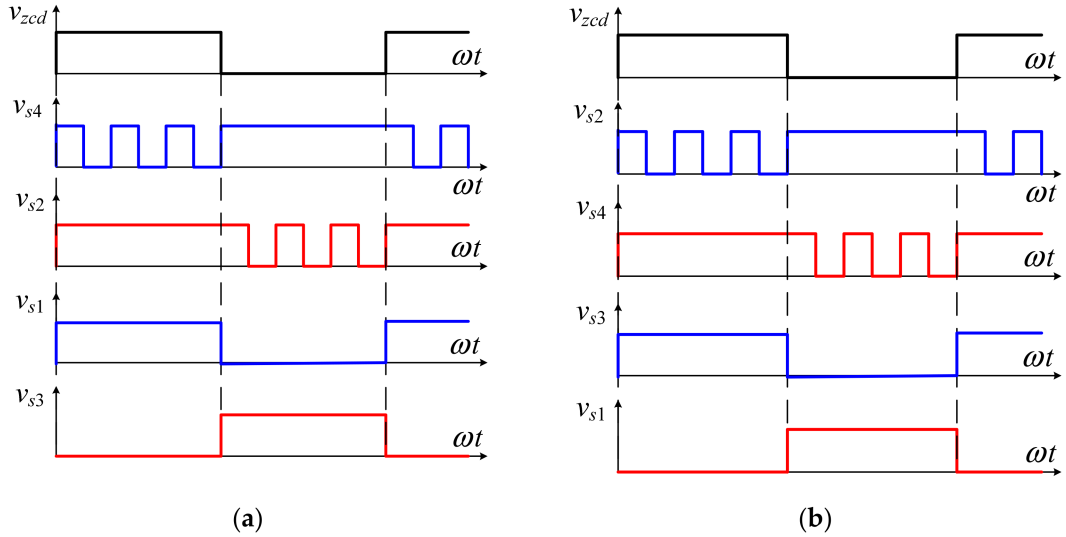

Figure 7. Switching control signals for (**a**) non-inverted output and (**b**) inverted output.

The details of the power transfer from input to output are explored in the highlighted loops of Figure 8a–d when the value of the input is positive and negative, respectively.

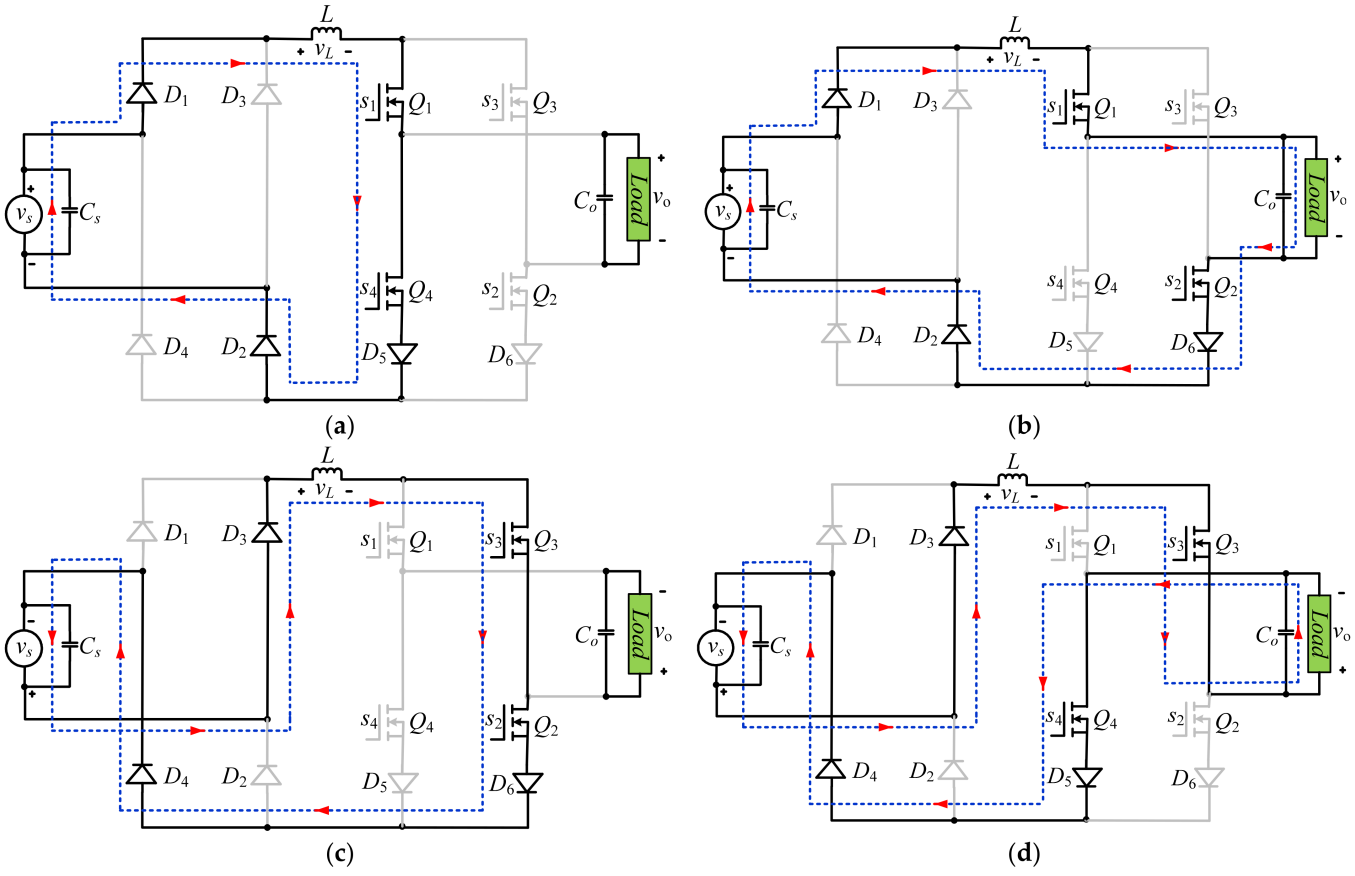

Figure 8. In-phase voltage boost operation during (**a**,**c**) shoot-through interval of positive and negative input voltage, respectively; (**b**,**d**) energy transfer interval of positive and negative input voltage, respectively.

For a positive input voltage, the diodes D_1 and D_2 are forward-biased, and the switching transistor Q_1 is on. The PWM switching of transistor Q_4 during the time interval 'kT', stores the input power in inductor 'L' through the current loop formed by the diodes D_1, D_2, and D_5 and switching transistors Q_1 and Q_4, as shown in Figure 8a. Here, 'k' and 'T' are the pulse width and switching period of the high-frequency PWM control signal, respectively. The peak reverse voltage across the reverse-biased diodes (D_3 and D_4) of the diode bridge is equal to the peak value of the input voltage.

$$V_{P(D_3,D_4)} = V_{s(P)} \tag{1}$$

Similarly, the maximum reverse voltage across the Q_3 and D_6 is the peak output voltage.

$$V_{P(D_6,Q_3)} = V_{o(P)} \tag{2}$$

In the 'kT' interval, although the switching transistor Q_2 is on, it is in the non-conducting state as its series-connected diode D_6 is reverse-biased due to the polarity of the output capacitor. This transistor is maintained in conduction mode to eliminate the possible interruption of the inductor's current as diode D_6 becomes forward once the switching transistor Q_4 turns off in the '$(1-k)\,T$' interval. During this interval, the stored power in the inductor is forwarded to the output through the power transfer loop highlighted in Figure 8b. The maximum voltage across the series-connected switching transistor Q_4 and diode D_5 is $V_{o(P)}$.

During the negative half-cycle of the input voltage, the operating states of diodes D_3 and D_4 are changed from off to on and diodes D_1 and D_2 become reverse-biased with a break-over value of peak input voltage. The operating transistor Q_3 conducts, and Q_1 remains reverse-biased. Its value cannot exceed the maximum output voltage level during the entire negative half-cycle of the input voltage. The regulation of the output voltage is ensured with the PWM control of the switching transistor Q_2. The voltage across the non-conducting devices can be described as follows:

$$V_{P(D_1,D_2)} = V_{s(P)} \tag{3}$$

$$V_{P(D_5,Q_1)} = V_{o(P)} \tag{4}$$

In the same voltage half-cycle, the turning on of the switching transistor Q_4 ensures the continuous inductor current as non-conducting diode D_5 that is connected in its series changes its operating state once the high-frequency PWM-controlled transistor Q_2 changes its switching state from 'on' to 'off'. During a PWM interval, the transfer of power from the source to the inductor and then to output is shown in Figure 8c,d, respectively. The dynamic variation in the inductor voltage and capacitor current is computed by employing Kirchhoff's voltage law (KVL) for the inductor voltage and Kirchhoff's current law (KCL) for the capacitor current, respectively. The inductor voltage and the capacitor current during the turn-on PWM intervals for any value of the supplied voltage are expressed by

$$L\frac{di_{id}}{dt} = kv_s \tag{5}$$

$$C_o\frac{di_c}{dt} = -ki_o \tag{6}$$

The inductor voltage and capacitor current during the turn-off PWM intervals for any value of the supplied voltage are as follows:

$$L\frac{di_{id}}{dt} = (k-1)v_o + (1-k)v_s \tag{7}$$

$$C_o\frac{di_o}{dt} = (1-k)i_s + (k-1)i_o \tag{8}$$

The derivative values of inductor current and capacitor voltage in steady-state conditions are negligible; the right-hand sides of Equations (5)–(8) are added, respectively, to obtain the voltage and current transfer ratio.

$$\frac{V_o}{V_s} = \frac{1}{1-k} \tag{9}$$

$$\frac{I_s}{I_o} = \frac{1}{1-k} \tag{10}$$

2.2. Voltage Control with Inverting Characteristics

The role of the front-end diode bridge remains similar as discussed for the non-inverting operation. It is an absolute value converter that transforms the sinusoidal input voltage to its absolute form. The peak voltage across the reverse-biasing diodes of this bridge cannot exceed the peak value of the input voltage. Thus, the diode bridge always delivers a time-varying unidirectional voltage at the input of the transistor's bridge. This voltage is transformed to a regulated bidirectional voltage with boost characteristics. For the inverting operation, the control process for switching transistors Q_1 and Q_3 is inverted, as can be seen in Figure 7b. The PWM behavior of switching transistor Q_4 for the non-inverting operation is changed to Q_2 for a positive input and vice versa for a negative input. This means that the PWM control of switching transistors Q_4 and Q_2 stabilizes the positive and negative output for non-inverting and inverting operations, respectively. Figure 9a–d illustrate the transfer of power for a positive and negative regulated output voltage.

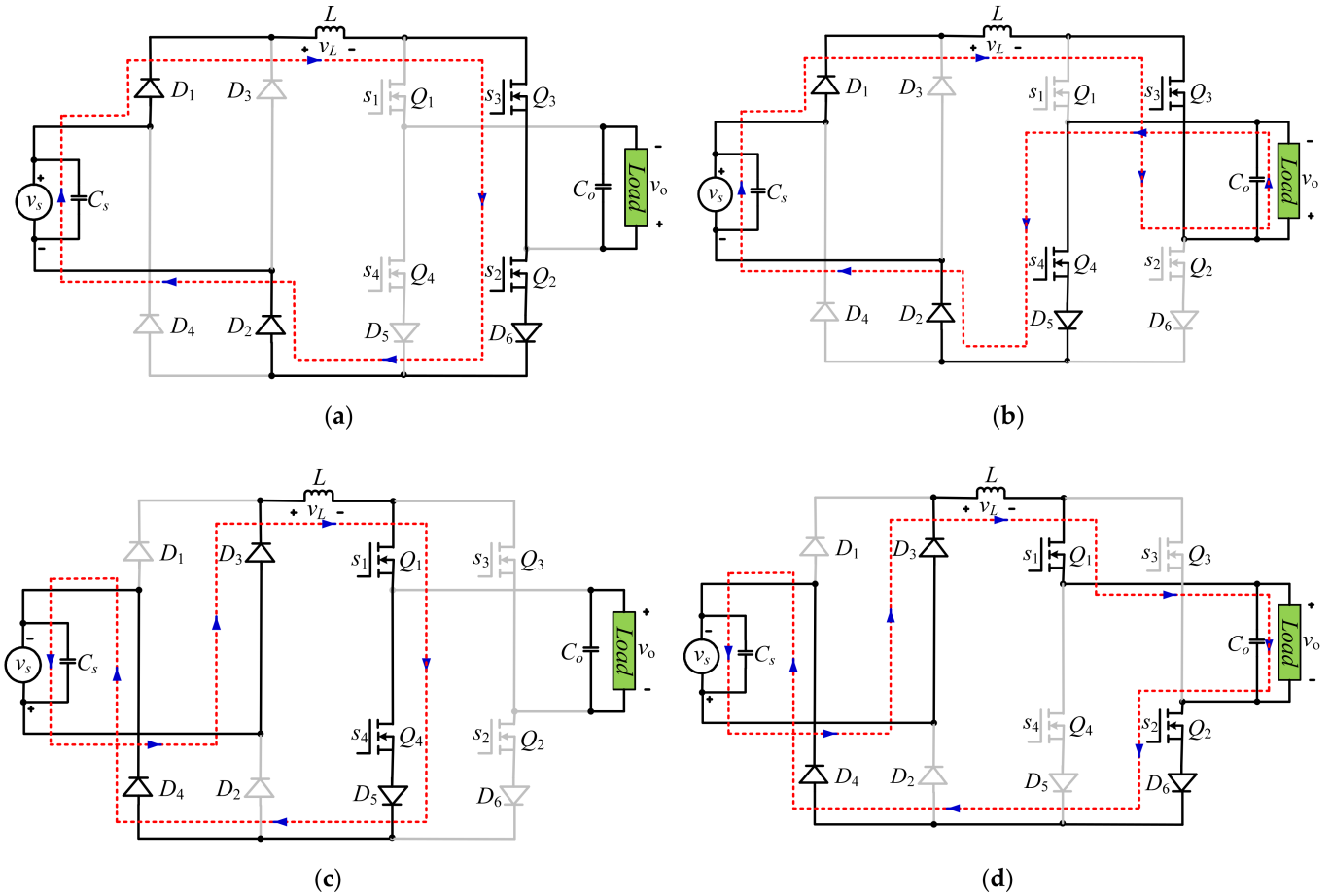

Figure 9. Out-phase voltage boost operation during (**a**,**c**) shoot-through interval of positive and negative input voltage, respectively; (**b**,**d**) energy transfer interval of positive and negative input voltage, respectively.

A similar approach as used for the non-inverting operation may be employed to compute the dynamic value of the inductor voltage and capacitor current during the PWM turn-on and -off period by using the KVL and KCL, respectively.

$$L\frac{di_{id}}{dt} = kv_s \tag{11}$$

$$C_o\frac{di_c}{dt} = -ki_o \tag{12}$$

$$L\frac{di_{id}}{dt} = (1-k)v_o + (1-k)v_s \tag{13}$$

$$C_o\frac{di_o}{dt} = (1-k)i_s + (k-1)i_o \tag{14}$$

The dynamic values of the inductor current and capacitor voltage during the steady-state condition can be ignored due to the low variation in the required output frequency. Thus, the right-hand sides of Equations (11)–(14) are added, respectively, to obtain the voltage and current transfer ratio.

$$\frac{V_o}{V_s} = \frac{-1}{1-k} \tag{15}$$

$$\frac{I_s}{I_o} = \frac{1}{1-k} \tag{16}$$

3. Comparative Analysis

The use of fewer (four) switching transistors and diodes (six) decreases the volume and cost of the converter. The control signal generated by any digital controller (microcontroller or processor) is not able to directly govern the switching states (on-to-off and off-to-on) of a switching transistor as their voltage level is as low (normally 0 to 5 V) as that of the power circuit. Thus, electrical isolation of the high-voltage side to a low voltage level is mandatory. For this purpose, the turn-on and turn-off control of a switching transistor requires the use of one gate-controlling (driving) circuit and one isolated DC source. The realization of a gate-controlling circuit is achieved by employing a hybrid chip along with many passive components and microelectronic devices. In the same way, the implementation of an isolated DC source needs a low-frequency step-down transformer, a bridge rectifier, and filtering components to smooth the output. Therefore, the size and cost of the gate-controlling circuit and isolated DC source are much larger than those of a switching transistor. The total volume and cost of the converter heavily depend on the number of switching transistors. In addition, the proposed topology requires fewer diodes as well. Thus, the elimination of diodes and switching transistors is the major achievement of the proposed circuit topology. A bipolar voltage gain boost converter, as reported in [20], is realized with the use of six switching transistors (six gate-controlling circuits and six isolated DC sources) and eight diodes. However, the developed circuit can be used to realize all outputs of [20] with the help of four transistors (four controlling circuits and isolated DC sources) and six diodes only. Therefore, the realization of the proposed topology drastically reduces the overall volume and cost.

It can be seen for any of the conducting intervals in all operating modes of Figures 8 and 9 that the operation of two switching transistors and three diodes realizes the required result. There is no change in the average conduction losses of the developed circuit and the circuit in [20]. Equation (17) illustrates the average conduction losses caused by one switching transistor and one diode. Here, 'V_d', 'R_d' and 'R_m' represent the forward voltage of the diode, forward resistance of the diode, and on-state resistance of the switching transistor, respectively.

$$P_{cond(diode+transistor)} = \frac{V_d I_{o(p)}}{\pi(1-k)} + \frac{I_{o(p)}^2}{4(1-k)^2}R_d + \frac{I_{o(p)}^2}{4(1-k)^2}R_m \tag{17}$$

In one cycle operation of the output voltage, four transistors and six diodes are to be conducted to realize the output. The total average conduction losses may be expressed as

$$P_{cond} = \frac{6V_d I_{o(p)}}{\pi(1-k)} + \frac{6I_{o(p)}^2}{4(1-k)^2}R_d + \frac{I_{o(p)}^2}{(1-k)^2}R_m \quad (18)$$

By employing the approach as used in [20], the average switching losses of a transistor and diode are calculated with the value of switching frequency (f_s) and reverse recovery charge (Q_{RR}).

$$P_{sw(transistor+diode)} = \frac{V_{o(p)} I_{o(p)} f_s (t_r + t_f)}{4(1-k)} + \frac{Q_{RR} V_{o(p)} f_s}{\pi} \quad (19)$$

It can be observed that switching losses are directly related to the switching frequency, so the switching losses of the low-frequency-operated diodes are negligible. In the proposed topology and the circuit in [20], there are only four conduction diodes (two for each half-cycle) at the high switching frequency. The total average switching losses can be computed as

$$P_{sw} = \frac{V_{o(p)} I_{o(p)} f_s (t_r + t_f)}{(1-k)} + \frac{4Q_{RR} V_{o(p)} f_s}{\pi} \quad (20)$$

In summary, the validation of the proposed converter is carried out by comparing its performance indexed with the existing converter realized with a similar approach, as can be seen in Table 1.

Table 1. Validation through comparison.

Comparing Parameters	Proposed Circuit	Circuit Reported in [20]
Used transistors	4	6
Used diodes	6	8
Gate-controlling circuits	4	6
Isolated DC sources	4	6
Bipolar voltage gain	symmetric $\left(\frac{\pm 1}{1-k}\right)$	symmetric $\left(\frac{\pm 1}{1-k}\right)$
Peak reverse voltage of the switching devices	$V_{o(P)}$	$V_{o(P)}$
Conducting transistors	2	2
Conducting diodes	3	3
Average conduction losses	$\frac{6V_d I_{o(p)}}{\pi(1-k)} + \frac{6I_{o(p)}^2}{4(1-k)^2}R_d + \frac{I_{o(p)}^2}{(1-k)^2}R_m$	$\frac{6V_d I_{o(p)}}{\pi(1-k)} + \frac{6I_{o(p)}^2}{4(1-k)^2}R_d + \frac{I_{o(p)}^2}{(1-k)^2}R_m$
Average switching losses	$\frac{V_{o(p)} I_{o(p)} f_s (t_r+t_f)}{(1-k)} + \frac{4Q_{RR} V_{o(p)} f_s}{\pi}$	$\frac{V_{o(p)} I_{o(p)} f_s (t_r+t_f)}{(1-k)} + \frac{4Q_{RR} V_{o(p)} f_s}{\pi}$

The comparative analysis of the suggested circuit with the circuit reported in [20] illustrates that the use of a smaller number of solid-state devices increases its potential to be applied as an AC voltage controller with a voltage having non-inverting and inverting capabilities.

4. Results and Discussion

For validation purposes, the waveforms of the output voltage and voltage across the various switching devices (transistors and diodes) are obtained by modeling the proposed circuit in a Simulink-based platform. Then, these plots are also compared and validated

with the practically obtained result as well. The details of the results obtained through the simulation-based platform and practical setup are detailed here.

4.1. Results Gained through Simulation Platform

The peak value of the input AC source is taken as 36 V (25 rms voltage) at 50 Hz frequency. The duty cycle of the PWM-controlled switching transistor is set to '0.4' to obtain a 60 V peak AC voltage at the output. The value of the switching frequency is set to 50 kHz. The diode is a model with 0.8 V forward voltage and 5 mΩ internal resistance. The internal resistance of the switching transistor is chosen to be 80 mΩ. Load resistance of 50 Ω is used to ensure safe currents for the switching devices. The internal parameters of the semiconductor devices (transistors and diodes) can be seen in the data sheets presented in the section containing the real results. The values of the input and output capacitors are set to 1 µF and 4.7 µF, respectively. A 1 mH value inductor is selected, which is inserted between the diode and transistor bridge.

The plots of the output voltage with respect to the input voltage are depicted in Figure 10a,b for voltage in-phase and out-of-phase operation. Here, the output voltages in both scenarios are almost two volts lower than their ideal value as some voltages are dropped internally in the semiconductor devices.

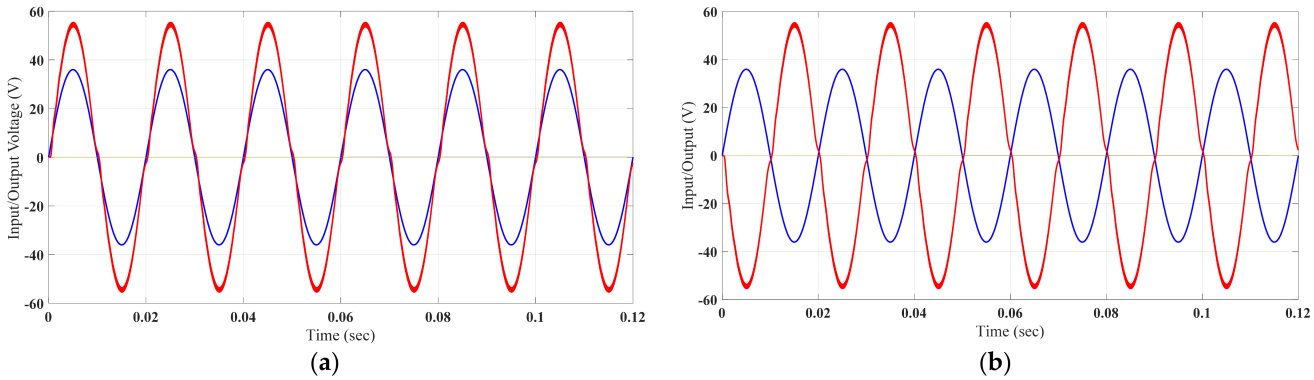

Figure 10. Simulation plotting input (blue) and output (red) during (**a**) non-inverting operation; (**b**) inverting operation.

In the same way, the value of the peak reverse voltage across the switching devices is verified through the simulation plots of Figure 11. Here, it can be observed that the maximum voltage across the switching devices of the transistor's bridge is raised to the output voltage level, while, in the case of the diode's bridge, it is restricted to only the input peak voltage level.

4.2. Results Gained through Practical Platform

A practical platform in the lab was developed with IRF 840 as a switching transistor and RHRG3040 as a diode. The turn-on and turn-off operation of IRF840 is supported by employing four gate-controlling circuits realized with hybrid chip EXB840 and four isolated DC sources. The values of the input voltage, switching frequency, and filtering components are the same as those used in the simulation. A high-speed STM microcontroller is employed for the generation of the control signals that are aligned with the variation in the input voltage. This is ensured by employing the output of a voltage-sensing circuit to the STM controller as a control input. All the practical waveforms are obtained by using a dual-channel RIGOL (DS1052E) oscilloscope.

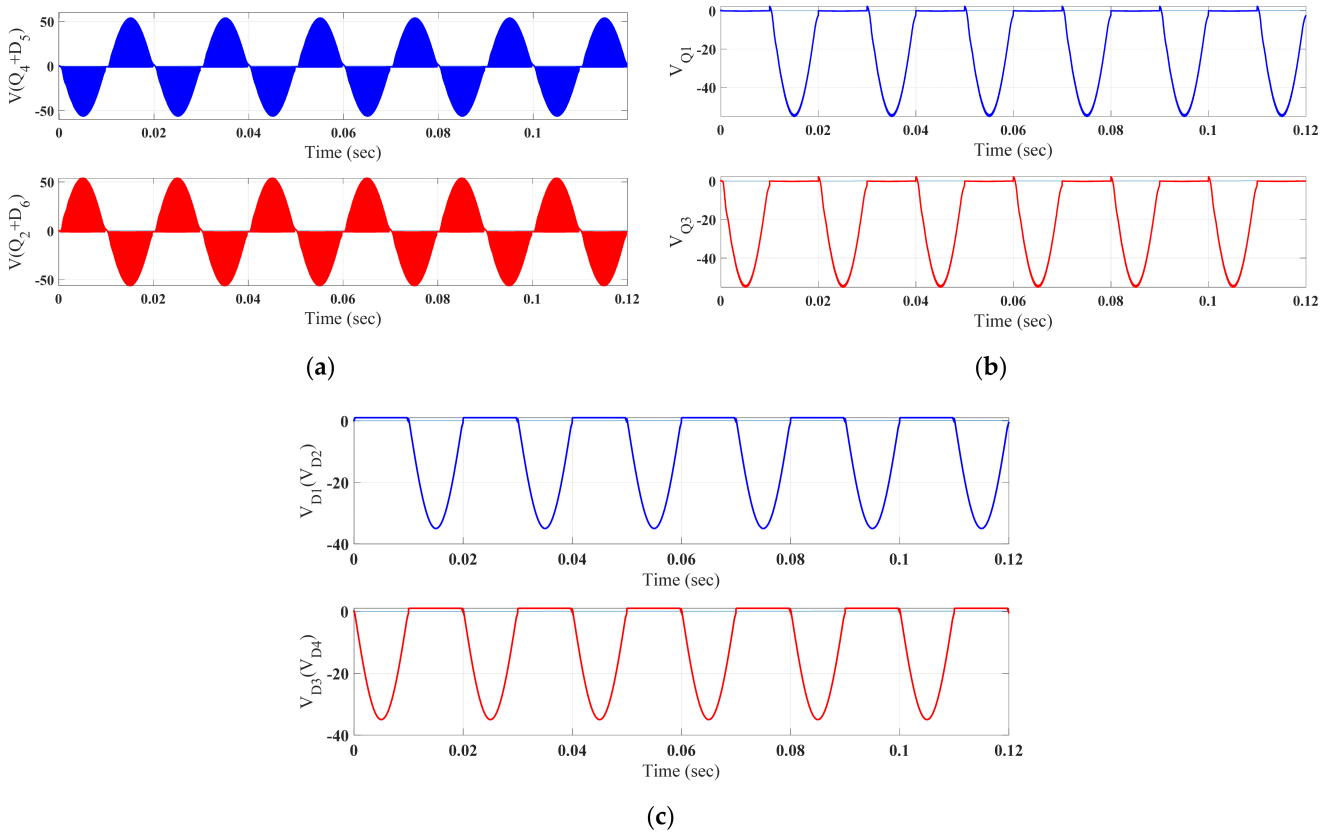

Figure 11. Simulated voltage waveforms developed across the semiconductor devices: (**a**) Q_4, D_5 (blue) and Q_4, D_5 (red); (**b**) Q_1 (blue) and Q_3 (red); (**c**) D_1, D_2 (blue) and Q_3, D_4 (red).

The recorded waveforms of Figure 12a,b from the practical platform confirm the non-inverting and inverting boost operation. The stabilization of the output voltage with either polarity of the voltage gain can be achieved by the PWM control. Similarly, the practical results of Figure 13a–c prove the validity of the peak inverse voltage that may be developed across the solid-state devices.

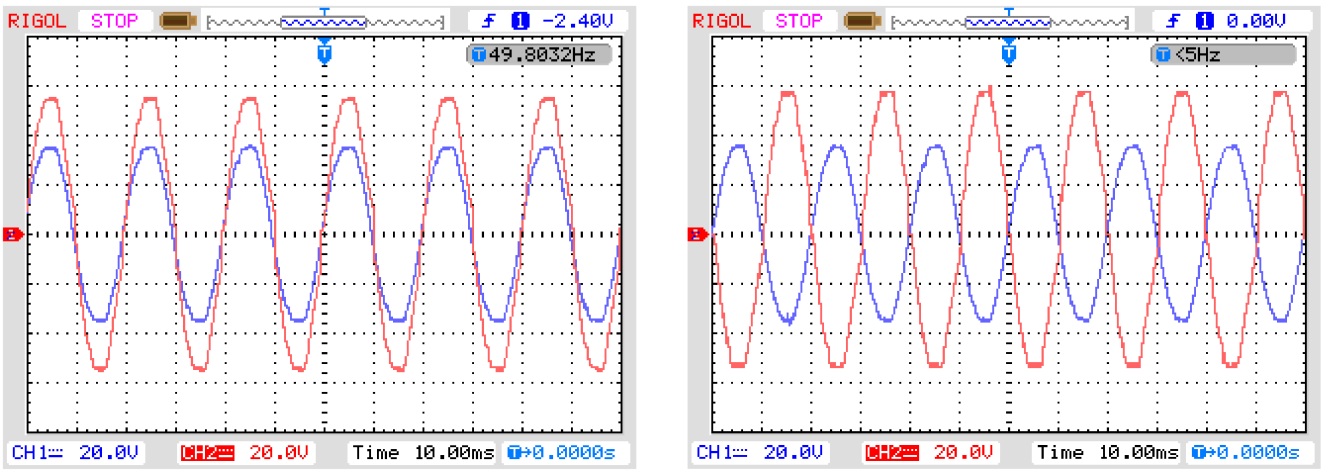

Figure 12. Practically gained waveforms of input (blue) and output (red) for (**a**) non-inverted output and (**b**) inverted output.

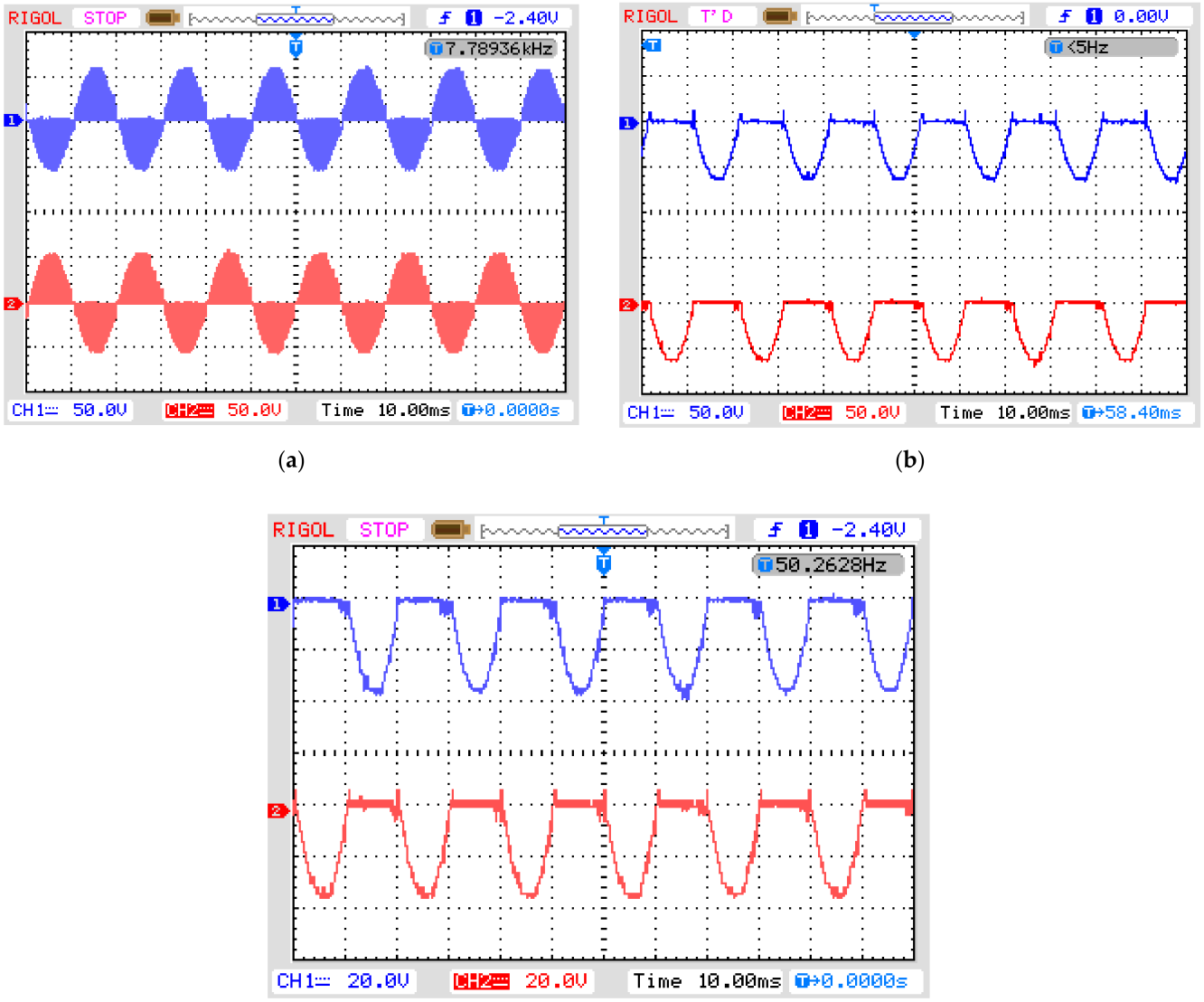

Figure 13. Practically gained voltage waveforms developed across the semiconductor devices: (**a**) Q_4, D_5 (blue) and Q_4, D_5 (red); (**b**) Q_1 (blue) and Q_3 (red); (**c**) D_1, D_2 (blue) and Q_3, D_4 (red).

5. Conclusions

This article focuses on developing a new AC voltage controller to obtain a bipolar output voltage with boost capabilities, realized by using only four switching transistors and six diodes. This output voltage capability may address the voltage sag and swell problem, which requires a high compensating voltage at the power distribution voltage level. The reduction in operating transistors compared to existing converters realized with a similar approach drastically reduces the circuit volume and cost because this is directly linked to the number of operating transistors. The operation of a high-frequency transistor requires the use of one gate-controlling circuit along with one isolated DC source. The overall size and cost of the gate-controlling circuit are normally greater than those of a switching transistor or power converter. The effectiveness of the proposed circuit was tested and verified with results obtained through Simulink modeling and a practically developed platform. These results confirm the theoretically computed values.

Author Contributions: Conceptualization, N.A. and G.A.; data curation, G.A. and N.U.; formal analysis, N.A., S.A.O. and U.F.; funding acquisition, N.U. and A.A.; investigation, N.A. and M.Z.; methodology, G.A. and A.A.; project administration, G.A.; resources, S.A.O. and N.U.; software, U.F. and M.Z.; validation, U.F. and M.Z.; writing—original draft, N.A. and G.A.; writing—review and editing, G.A., S.A.O. and N.U. All authors have read and agreed to the published version of the manuscript.

Funding: This research work was supported by Taif University Researchers Supporting Project number (TURSP-2020/228), Taif University, Taif, Saudi Arabia.

Institutional Review Board Statement: Not applicable.

Informed Consent Statement: Not applicable.

Data Availability Statement: Not applicable.

Acknowledgments: The authors acknowledge the financial support from Taif University Researchers Supporting Project Number (TURSP-2020/228), Taif University, Saudi Arabia. The authors are also thankful to the Department of Electrical Engineering, the University of Lahore, Pakistan for providing the facilities to conduct this research.

Conflicts of Interest: The authors declare no conflict of interest.

References

1. Abas, N.; Dilshad, S.; Khalid, A.; Saleem, M.S.; Khan, N. Power Quality Improvement Using Dynamic Voltage Restorer. *IEEE Access* **2020**, *8*, 164325–164339. [CrossRef]
2. Zheng, Z.-X.; Xiao, X.-Y.; Chen, X.Y.; Huang, C.-J.; Zhao, L.-H.; Li, C.-S. Performance Evaluation of a MW-Class SMES-BES DVR System for Mitigation of Voltage Quality Disturbances. *IEEE Trans. Ind. Appl.* **2018**, *54*, 3090–3099. [CrossRef]
3. de Almeida Carlos, G.A.; Jacobina, C.B. Series Compensator Based on Cascaded Transformers Coupled With Three-Phase Bridge Converters. *IEEE Trans. Ind. Appl.* **2017**, *53*, 1271–1279. [CrossRef]
4. Fernandes, D.A.; Costa, F.F.; Martins, J.R.; Lock, A.S.; da Silva, E.R.; Vitorino, M.A. Sensitive Load Voltage Compen-sation Performed by a Suitable Control Method. *IEEE Trans. Ind. Appl.* **2017**, *53*, 4877–4885. [CrossRef]
5. Dilshad, S.; Abas, N.; Farooq, H.; Kalair, A.R.; Memon, A.A. NeuroFuzzy Wavelet Based Auxiliary Damping Controls for STATCOM. *IEEE Access* **2020**, *8*, 200367–200382. [CrossRef]
6. Chen, C.I.; Chen, Y.C.; Chen, C.H.; Chang, Y.R. Voltage Regulation Using Recurrent Wavelet Fuzzy Neural Network-Based Dynamic Voltage Restorer. *Energies* **2020**, *13*, 6242. [CrossRef]
7. Torres, A.P.; Roncero-Sanchez, P.; Vazquez, J.; Lopez-Alcolea, F.J.; Molina-Martinez, E.J. A Discrete-Time Control Method for Fast Transient Voltage-Sag Compensation in DVR. *IEEE Access* **2019**, *7*, 170564–170577. [CrossRef]
8. Jimichi, T.; Fujita, H.; Akagi, H. Design and Experimentation of a Dynamic Voltage Restorer Capable of Significantly Re-ducing an Energy-Storage Element. *IEEE Trans. Ind. Appl.* **2008**, *44*, 817–825. [CrossRef]
9. Peng, F.Z.; Chen, L.; Zhang, F. Simple topologies of PWM AC-AC converters. *IEEE Power Electron. Lett.* **2003**, *1*, 10–13. [CrossRef]
10. Fang, X.P.; Qian, Z.M.; Peng, F.Z. Single-phase Z-source PWM AC-AC converters. *IEEE Power Electron. Lett.* **2005**, *3*, 121–124. [CrossRef]
11. Nguyen, M.-K.; Lim, Y.C.; Kim, Y.-J. A Modified Single-Phase Quasi-Z-Source AC–AC Converter. *IEEE Trans. Power Electron.* **2011**, *27*, 201–210. [CrossRef]
12. He, L.; Nai, J.; Zhang, J. Single-Phase Safe-Commutation Trans-Z-Source AC–AC Converter with Continuous Input Current. *IEEE Trans. Ind. Electron.* **2017**, *65*, 5135–5145. [CrossRef]
13. Aleem, Z.; Yang, H.-K.; Ahmed, H.F.; Winberg, S.L.; Park, J.-W. A Class of Single-Phase Z-Source AC–AC Converters with Magnetic Coupling and Safe-Commutation Strategy. *IEEE Trans. Ind. Electron.* **2021**, *68*, 8104–8115. [CrossRef]
14. Ahmed, H.F.; Cha, H. A New Class of Single-Phase High-Frequency Isolated Z-Source AC–AC Converters with Reduced Passive Components. *IEEE Trans. Power Electron.* **2017**, *33*, 1410–1419. [CrossRef]
15. Ahmed, H.F.; Cha, H.; Khan, A.A.; Kim, J.; Cho, J. A Single-Phase Buck–Boost Matrix Converter with Only Six Switches and Without Commutation Problem. *IEEE Trans. Power Electron.* **2016**, *32*, 1232–1244. [CrossRef]
16. Ashraf, N.; Abbas, G.; Abbassi, R.; Jerbi, H. Power Quality Analysis of the Output Voltage of AC Voltage and Frequency Controllers Realized with Various Voltage Control Techniques. *Appl. Sci.* **2021**, *11*, 538. [CrossRef]
17. Ashraf, N.; Abbas, G.; Khan, I.; Raza, A.; Ullah, N. A Transformer-Less Multiconverter Having Output Voltage and Fre-quency Regulation Characteristics, Employed with Simple Switching Algorithms. *Apll. Sci.* **2021**, *11*, 3075. [CrossRef]
18. Ashraf, N.; Izhar, T.; Abbas, G. A Single-Phase Buck-Boost Matrix Converter with Low Switching Stresses. *Math. Probl. Eng.* **2019**, *2019*, 1–19. [CrossRef]
19. Ashraf, N.; Izhar, T.; Abbas, G.; Awan, A.B.; Farooq, U.; Balas, V.E. A New Single-Phase AC Voltage Converter with Voltage Buck Characteristics for Grid Voltage Compensation. *IEEE Access* **2020**, *8*, 48886–48903. [CrossRef]

20. Ashraf, N.; Abbas, G.; Ullah, N.; Alkhammash, H.I.; Zubair, M. An Improved Bipolar Voltage Boost AC Voltage Controller with Reduced Switching Transistors. *IEEE Access* **2021**, *9*, 1. [CrossRef]
21. Subramanian, S.; Mishra, M. Interphase AC–AC Topology for Voltage Sag Supporter. *IEEE Trans. Power Electron.* **2009**, *25*, 514–518. [CrossRef]
22. Sharifi, S.; Monfared, M.; Babaei, M.; Pourfaraj, A. Highly Efficient Single-Phase Buck–Boost Variable-Frequency AC–AC Converter with Inherent Commutation Capability. *IEEE Trans. Ind. Electron.* **2019**, *67*, 3640–3649. [CrossRef]
23. Ahmed, H.F.; El Moursi, M.S.; Zahawi, B.; Al Hosani, K. A High-Frequency Isolated Multilevel Cascaded-Type Bipolar Direct PWM AC–AC Converter for Utility Voltage Compensation. *IEEE Trans. Ind. Appl.* **2021**, *57*, 3188–3201. [CrossRef]
24. Ahmed, H.F.; El Moursi, M.S.; Zahawi, B.; Al Hosani, K.; Khan, A.A. Single-Phase Symmetric-Bipolar-Type High-Frequency Isolated Buck-Boost AC–AC Converter With Continuous Input and Output Currents. *IEEE Trans. Power Electron.* **2021**, *36*, 11579–11592. [CrossRef]
25. Ashraf, N.; Abbas, G.; Ullah, N.; Alahmadi, A.A.; Awan, A.B.; Zubair, M.; Farooq, U. A Simple Two-Stage AC-AC Circuit Topology Employed as High-Frequency Controller for Domestic Induction Heating System. *Appl. Sci.* **2021**, *11*, 8325. [CrossRef]